Structural corneal changes identified with the use of confocal microscopy after accelerated CXL for keratoconus

L.F. Troichenko[1], Cand Sc (Med); **K.V. Sereda**[1], Cand Sc (Med); **G.I. Drozhzhyna**[1], Dr Sc (Med); **O.M. Ivanova**[1], Cand Sc (Med); **N.V. Medvedovska**[2], Dr Sc (Med), Prof.

[1] Filatov Institute of Eye Diseases and Tissue Therapy, NAMS of Ukraine;

Odesa (Ukraine)

[2] P.L. Shupyk National Medical Academy of Postgraduate Education;

Kyiv (Ukraine)

E-mail: cornea@te.net.ua

Keywords

keratoconus, corneal collagen, accelerated cross-linking

Background: *Post-crosslinking (CXL) biomicroscopic changes in patients with keratoconus can be detected by confocal microscopy. Few studies reported on morphological changes in the cornea after CXL.*

Purpose: *To detect structural corneal changes by confocal microscopy after accelerated CXL for keratoconus.*

Material and Methods: *This study included 119 patients (167 eyes) who underwent accelerated CXL for keratoconus and were followed up for 12 months. Accelerated CXL was carried out using the UV-X™ 2000 Crosslinking System at an irradiation intensity of 9 mW/ cm². Confocal biomicroscopy was performed using the Confoscan 4 unit (NIDEK Co., Ltd., Aichi, Japan).*

Results: *Accelerated CXL (carried out in 10 minutes) for stage 2 to 3 progressive keratoconus is safe and allows stabilizing the pathological process, based on the 12-month follow-up results. At 3 months after accelerated CXL, active regeneration of keratocytes was seen in the superficial and deep stroma, with resolution of fibrotic foci. Confocal microscopy found that recovery of normal corneal architectonics started at 6 months and keratocyte repopulation was complete at 12 months after CXL.*

Introduction

Keratoconus (KCN) is a corneal dystrophy that is characterized by structural changes in the cornea leading to progressive corneal thinning and bulging, which is accompanied by the development of irregular astigmatism and substantially decreased visual acuity [1-5].

Corneal collagen crosslinking (CXL) is generally regarded as the gold standard for treating progressive stage 2 to 3 keratoconus [6]. Photochemical ionization takes place and riboflavin is destroyed (with release of free oxygen) by exposure to UV-A radiation generated by the UV-X system. Free oxygen-derived radicals cause cross-linking between -CH and –CN groups in collagen molecules, which induces their binding to form a 3D meshwork. Numerous additional bounds between corneal collagen fibers result in a significant improvement of corneal mechanical strength and rigidity. Biomechanical studies have shown that corneal rigidity increases by 350%-380% after cross-linking [6-11].

Post-crosslinking biomicroscopic corneal changes in keratoconic eyes can be detected by confocal microscopy.

Confocal corneal microscopy is an up-to-date technique enabling in vivo corneal monitoring with tissue cell and microstructural imaging.

Clinical use of confocal corneal microscopy allowed moving to a new level of in vivo dynamic imaging of corneal ultrastructural changes of various etiology [12-15]. Quantitative composition of corneal cell layers is an important characteristic of the state of the cornea [16].

The list of corneal dystrophies and degenerations studied with confocal microscopy includes epithelial basement membrane dystrophies, Reis-Bucklers corneal dystrophy, Meesmann corneal dystrophy, lattice corneal dystrophy, granular corneal dystrophy, spotted corneal dystrophy, Schnyder crystalline corneal dystrophy, posterior polymorphous corneal dystrophy, Fuchs' endothelial corneal dystrophy (or cornea guttata), keratoconus, iridocorneal endothelial syndrome, Salzmann's corneal degeneration, retrocorneal membrane and primary corneal amyloidosis [15, 17-28].

Confocal microscopy allows for early disease diagnosis, differential diagnosis between various corneal disorders, and control of therapeutic and surgical treatment efficacy.

Confocal microscopy studies have demonstrated substantial qualitative and quantitative changes in all corneal layers in keratoconic eyes. Thus, in vivo confocal microscopy (IVCM) allows for detecting morphological corneal changes as early as the subclinical stage of keratoconus [29].

Confocal microscopy studies by Hollingsworth et al [30] and Somodi et al [13] noted a substantially increased size of hyperreflecting epithelial cells and irregularly arranged superficial epithelial cells in keratoconic eyes. In addition, it has been demonstrated that desquamated epithelial cells are characteristic for keratoconic eyes. The central cornea of subjects with keratoconus and age-matched control subjects was assessed using IVCM and corneal aesthesiometry, and significant differences in corneal nerve fibre density were found between the former subjects and latter subjects [16, 31]. Keratoconic corneas exhibited abnormal sub-basal nerve architecture compared with patterns previously observed in normal corneas [32-34]. Keratoconus corneal stroma is always involved in the pathological process, with a decreased number of keratocytes that are irregularly arranged in the posterior stroma. As the disease progresses, microstriae appear as diverse hyporeflective thin lines [35].

Confocal miscroscopy found loss of the subbasal nerve plexus and a reduced number of anterior stromal keratocytes in early postoperative period (< 1 month) after treatment of progressive keratoconus by riboflavin-UVA-induced CXL. This may be observed clinically as temporary stromal corneal haze with edema. The regeneration of keratocytes starts at 3 months and is complete at 6 months after CXL [36, 37].

A few studies reported on morphological changes in the cornea after CXL performed with the Dresden protocol and after accelerated CXL (ACXL). Mazzotta et al [37] noted regeneration of the subbasal nerve plexus and restored keratocyte density at 12 months after CXL.

The purpose of this study was to detect structural corneal changes after accelerated CXL for keratoconus.

Material and Methods

One hundred and nineteen patients (167 eyes; 90 men and 29 women) aged 12-57 years (25.3 ± 8.55 SD years; median value, 25 years) who underwent ACXL for keratoconus were included in this study. Of these eyes, 77 (46.1%) had stage II keratoconus, and 90 (53.9 %) had stage III keratoconus (Amsler-Krumeich classification).

Accelerated CXL was carried out using the UV-X™ 2000 Crosslinking System (IROC Innocross, Zurich, Switzerland) at an irradiation intensity of 9mW/cm². Patients underwent biomicroscopy, refractometry, and corneal confocal biomicroscopy (Confoscan 4, NIDEK Co., Ltd., Aichi, Japan) in addition to a routine eye examination. Pentacam® apparatus (Oculus Inc., Wetzlar, Germany) was used to perform keratography and corneal pachymetry and to estimate corneal refractive power. Kmax was used as a measure of corneal refractive power, and thinnest local corneal thickness was measured.

Patients were followed up for 12 months after accelerated CXL procedure.

Results

The data below are arranged in the order of detected changes in corneal layers.

In the early postoperative period, confocal corneal biomicroscopy findings included epitheliopathy (with an increased number of desquamated epithelial cells). In addition, on confocal biomicroscopy images, epithelial cell nuclei appeared brighter than the surrounding cytoplasm. Moreover, basal epithelial cells were polymorphic, and varied both in size and in brightness (Fig. 1).

Confocal microscopy showed varying amounts of hyperreflectivity in the Bowman membrane, indicating active keratocyte regeneration. Transparency of the Bowman membrane was found to be restored at 1 month after accelerated CXL (Figs. 2, 3).

At day 2 after accelerated CXL, there were bright flares in collagen crosslinking region corresponding to the area of stromal fibroblastic metaplasia (Fig. 4). At day 7 after accelerated CXL, apoptotic keratocytes appeared in the anterior stromal layers in a honeycomb pattern, indicating the presence of a lacunar edema around them (Figs. 5, 6), but keretocyte nuclei were not visualized.

Of the 167 eyes, 9 (5.4%) had temporary complications in the form of corneal haze (superficial corneal stromal clouding) in the postoperative period. The haze disappeared and corneal transparency restored at day 6 or 7 after accelerated CXL.

At 1 month after accelerated CXL, the epitheliopathy findings disappeared, epithelial cells were seen with distinct margins, and decreased cell polymorphism. A lacunar stromal edema around keratocytes decreased, which was reflected by a decrease in meshwork size (Fig. 7 a,b). The stroma became more homogenous, active kerastocytes appeared, but there were still foci of hypocellularity and isolated Langerhans cells were seen.

At 3 months after accelerated CXL, active regeneration of keratocytes was seen in the superficial and deep stroma, with resolution of fibrotic foci (Fig. 8). At 6 months after accelerated CXL, regeneration of stromal structure was noted, and stromal folds were visible with limited focal non-intensive hyperreflectivity in the region of crosslinking (Fig. 9).

In addition, at 6 months, the following changes were observed clinically: (1) in all patients, epithelized superficial cornea, transparent stroma, and normal endothelium were seen on biomicroscopy, and (2) no statistically significant corneal thinning was observed. Mean thinnest local corneal thickness decreased from 459.7±36.6 SD μm (median value, 454.0 μm) at baseline to 456.5±37.1 SD μm (median value, 450.0 μm) at 6 months ($p > 0.1$).

At 12 months, corneal structure approached the norm, isolated active keratocytes were seen, and hyperreflective focus was mildly apparent (Fig. 10).

No changes in the posterior stromal layers and endothelium were found during the follow-up period.

Evenly epithelized superficial cornea, transparent stroma and normal endothelium were seen on biomicroscopy. Compared to baseline, the clinical findings at 12 months were as follows: (1) mean astigmatism

decreased from 4.16 ± 2.11(SD) D to 3.79 ± 2.56 (SD) D, (2) corneal refractive power as assessed by Kmax decreased significantly (p = 0.000) by 1.9 D to 55.9±6.93(SD) D (median value, 55.0 D); and (3) mean thinnest local corneal thickness did not change from baseline 453.7 ± 55.5(SD) μm (median value, 455 μm).

In addition, ninety percent of patients self-reported improvements in both vision quality and tolerance of refractive correction with spectacles.

Discussion

Touboul and colleagues [38] compared early corneal healing following conventional, transepithelial, and accelerated CXL protocols. In vivo corneal confocal microscopy analysis of the postoperative impact of CXL on the cornea revealed clear differences among these protocols. Accelerated CXL had a greater impact than conventional CXL on the anterior cornea, with stromal changes including increased tissue reflectivity, complete obliteration of keratocytes, and a honeycomb appearance. Transepithelial CXL, however, did not appear to alter corneal morphology [38].

Mazzotta and colleagues [36-37] demonstrated that that despite a significant decrease in the mean density of anterior keratocytes in the first 6 postoperative months, cell density after CXL and ACXL returned to baseline values at 12 months. In addition, IVCM of the endothelium and limbal structures showed no evidence of pathological changes.

Hyperreflective keratocytes in the anterior stroma indicate an active metabolic process and corneal stromal healing, and cause stromal haze that is seen on biomicroscopy. Temporary haze of the anterior-mid stroma after CXL represents an indirect sign of CXL-induced stromal collagen compaction and remodeling, and disappears 1 to 3 months after CXL [36-37].

Touboul and co-authors [38] noted that the central corneal subbasal nerve plexus corresponding to the crosslinking region was not visualized on confocal microscopy after CXL. These findings were confirmed by others [13, 31, 39-40] and point to the appearance of corneal re-innervation at 6 months after CXL. In line with these studies, the present study found gradual regeneration of the subbasal nerve plexus during the follow-up period, although the plexus was not distinctly visualized at 6 months after CXL.

Knappe and colleagues [41] noted that, early after CXL, the most prominent structural changes revealed by confocal microscopy were seen in the anterior-to-mid corneal stroma. Our research found a significant decrease in density of the anterior stroma after accelerated CXL, with gradual keratocyte repopulation starting at 6 months and a complete restoration of their population at 12 months after CXL; this was in line with findings of others [42-45].

This study found a significant difference neither in the number nor in the increase in size of corneal endothelial cells between baseline and 12 months after accelerated CXL time points, which was in agreement with previous studies [47-48].

Therefore, our accelerated CXL for stage 2 to 3 progressive keratoconus made it possible to stabilize the pathological process in 100% of cases, based on the 12-month follow-up results. Keratoconus stabilization was accompanied by: a decrease of astigmatism to 3.79 ± 2.56(SD) D and of the corneal refractive power by 1.9D; an increase of the corneal thickness by 8.8 nm; and recovery of corneal thickness to baseline values (453.7 ± 55.5(SD) μm). In addition, confocal microscopy found that recovery of normal corneal architectonics started at 6 months and was complete at 12 months after CXL.

Conclusion

First, accelerated CXL (carried out in 10 minutes) for stage 2 to 3 progressive keratoconus is safe and allows stabilizing the pathological process, based on the 12-month follow-up results. Second, confocal microscopy found that recovery of normal corneal architectonics started at 6 months and keratocyte repopulation was complete at 12 months after CXL.

References

1. Bikbov MM, Surkova VK. [Corneal collagen crosslinking for keratoconus]. A review. Ophthalmology in Russia. 2014;11(3):13-8. https://doi.org/10.18008/1816-5095-2014-3-13-19. Russian.
2. Birich TA, Chekina AIu, Aksionova NI. [Outcomes of treatment for keratoconus]. Oftalmologiia Belorusi. 2010;1(4):90-7. Russian.
3. Ivanovskaia EV, Vit VV, Golovchenko VG. [Immunological status of patients with various stages of keratoconus and keratoglobus]. Oftalmol Zh. 2000;5:40-4. Russian.
4. Sevastiianov EN, Gorskova EN, Ekgard VF. [Keratoconus (etiology, pathogenesis, medicinal treatment): textbook]. Cheliabinsk: UGMADO;2005. Russian.
5. Solodkova EG, Remesnikov IA. [Modern approaches in the treatment progressive keratectasia]. Prakticheskaia meditsina. 2012;4:75-9. Russian.
6. Adel Alhayek, Pei-Rong Lu. Corneal collagen crosslinking in keratoconus and other eye disease. Int J Ophthalmol. 2015; 8(2): 407–18. doi: 10.3980/j.issn.2222-3959.2015.02.35.
7. Kohlhaas M, Spoerl E, Schilde T, et al. Biomechanical evidence of the distribution of cross-links in corneas treated with riboflavin and ultraviolet A light. J Cataract Refract Surg. 2006 Feb;32(2):279-83.
8. Nowak DM, Gajecka M. The genetics of keratoconus. Middle East Afr J Ophthalmol. 2011 Jan;18(1):2-6. doi: 10.4103/0974-9233.75876.
9. Spoerl E, Mrochen M, Sliney D, et al. Safety of UVA – riboflavin cross – linking of the cornea. Cornea. 2007 May;26(4):385-9.
10. Sporl E, Huhle M, Kasper M, Seiler T. [Increased rigidity of the cornea caused by intrastromal crosslinking]. Ophthalmologe. 1997 Dec;94(12):902-6. German.
11. Vinciguerra P, Torres I, Camesasca FI. Applications of confocal microscopy in refractive surgery. J Refract Surg. 2002 May-Jun;18(3 Suppl):S378-81.
12. Cavanagh HD, Petroll WM, Alizadeh H, et al. Clinical and diagnostic use of in vivo confocal microscopy in patients with corneal disease. Ophthalmology. 1993 Oct;100(10):1444-54.

13. Somodi S, Hahnel C, Slowik C, et al. Confocal in vivo microscopy and confocal laser-scanning fluorescence microscopy in keratoconus. Ger J Ophthalmol. 1996 Nov;5(6):518-25.
14. Tsubota K, Mashima Y, Murata H, et al. Corneal epithelium in keratoconus. Cornea. 1995 Jan;14(1):77-83.
15. Vinciguerra P, Albè E, Trazza S, Rosetta P, Vinciguerra R, Seiler T, et al. Refractive, topographic, tomographic, and aberrometric analysis of keratoconic eyes undergoing corneal cross-linking. Ophthalmology. 2009 Mar;116(3):369-78. doi: 10.1016/j.ophtha.2008.09.048.
16. Patel SV, McLaren JW, Hodge DO, et al. Normal human keratocyte density and corneal thickness measurement by using confocal microscopy in vivo. Invest Ophthal Vis Sci. 2001 Feb;42(2):333-9.
17. Chew SJ, Beuerman RW, Assouline M, et al. Early diagnosis of infectious keratitis with in vivo real time confocal microscopy. CLAO J. 1992 Jul;18(3):197-201.
18. Chiou AG, Beuerman RW, Kaufman SC, Kaufman HE. Confocal microscopy in lattice corneal dystrophy. Graefes Arch Clin Exp Ophtalmol. 1999 Aug;237(8):697-701.
19. Chiou AG, Kaufman SC, Beuerman RW, et al. Confocal microscopy in posterior polymorphous corneal dystrophy. Ophthalmologica. 1999;213(4):211-3.
20. Ciancaglini M, Carpineto P, Doronzo E, et al. Morphological evaluation of Schnyder's central crystalline dystrophy by confocal microscopy before and after phototherapeutic keratectomy. J Cataract Refract Surg. 2009 Apr;37(3):308-12. doi: 10.1111/j.1442-9071.2009.02021.x.
21. Croghale NS. Epidemiology of keratoconus. Indian J Ophthalmol. 2013;61(8): 382-3.
22. Ku JY, Grupcheva CN, McGhee CN. Microstructural analysis of Salzmann's nodular degeneration by in vivo confocal microscopy. Clin Exp Ophtalmol. 2002 Oct;30(5):367-8.
23. Kymionis GD, Portaliou DM, Bouzoukis DI, et al. Herpetic keratitis with iritis after corneal crosslinking with riboflavin and ultraviolet A for keratoconus. J Cataract and Refract Surg. 2007 Nov;33(11):1982-4.
24. Rosenberg ME, Tervo TM, Muller LJ, et al. In vivo confocal microscopy after herpes keratitis. Cornea. 2002 Apr;21(3):265-9.
25. Rosenberg ME, Tervo TM, Immonen IJ, et al. Corneal structure and sensitivity in type 1 diabetes mellitus. Invest Ophthalmol Vis Sci. – 2000;41:2915–21.
26. Rothstein A, Auran J, Wittpenn J. et al. Confocal microscopy in Meretoja syndrome. Cornea. 2002 May;21(4):364-7.
27. Spoerl E, Huhle M, Seiler T. Induction of cross-links in corneal tissue. Exp Eye Res. 1998 Jan;66(1):97-103.
28. Spoerl E, Seiler T J. Techniques for stiffening the cornea. Refract Surg. 999 Nov-Dec;15(6):711-3.
29. Brookes NH, Loh IP, Clover GM, et al. Involvement of corneal nerves in the progression of keratoconus. Exper Eye Res. 2003;77:515–24.
30. Hollingsworth JG, Efron N, Tullo AB. In vivo corneal confocal microscopy in keratoconus. Ophthalmic Physiol Opt. 2005 May;25(3):254-60.
31. Simo Mannion L, Tromans C, O'Donnell C. An evaluation of corneal nerve morphology and function in moderate keratoconus. Cont Lens Anterior Eye. 2005 Dec;28(4):185-92. Epub 2005 Nov 21.
32. Patel DV, McGhee CN. Mapping the corneal sub-basal nerve plexus in keratoconus by in vivo laser scanning confocal microscopy. Invest Ophthalmol Vis Sci. 2006;47:1348–51.
33. Rabinowitz YS. Keratoconus. Surv Ophthalmol. 1998 Jan-Feb;42(4):297-319.
34. McQuaid R, Cummings AB, Mrochen M. The theory and art of corneal cross-linking. Indian J Ophthalmol. 2013 Aug;61(8):416-9.
35. Avetisov SE, Egorov EA, Moshetova LK, et al. [Ophthalmology: National Guidance]. GEOTAR-Media: Moscow; 2018. Russian.
36. Mazzotta C, Traversi C, Baiocchi S, Caporossi O, Bovone C, Sparano MC, et al. Corneal healing after riboflavin ultraviolet-A collagen cross-linking determined by confocal laser scanning microscopy in vivo: Early and late modifications. Am J Ophthalmol. 2008 Oct;146(4):527-533. doi: 10.1016/j.ajo.2008.05.042.
37. Mazzotta C, Hafezi F, Kymionis G, et al. In Vivo Confocal Microscopy after Corneal Collagen Crosslinking. Ocul Surf. 2015 Oct;13(4):298-314. doi: 10.1016/j.jtos.2015.04.007.
38. Touboul D, Efron N, Smadja D, et al. Corneal confocal microscopy following conventional, transepithelial, and accelerated corneal collagen cross-linking procedures for keratoconus. J Refract Surg. 2012 Nov;28(11):769-76. doi: 10.3928/1081597X-20121016-01.
39. Zare MA, Mazloumi M, Farajipour H, et al. Effects of corneal collagen crosslinking on confocal microscopic findings and tear indices in patients with progressive keratoconus. Int J Prev Med. 2016 Dec; 23(7): 132. doi: 10.4103/2008-7802.196527.
40. Wasilewski D, Mello GH, Moreira H. Impact of collagen crosslinking on corneal sensitivity in keratoconus patients. Cornea. 2013 Jul;32(7):899-902. doi: 10.1097/ICO.0b013e31827978c8.
41. Knappe S, Stachs O, Zhivov A, et al. Results of confocal microscopy examinations after collagen cross-linking with riboflavin and UVA light in patients with progressive keratoconus. Ophthalmologica. 2011;225(2):95-104. doi: 10.1159/000319465.
42. Macsai MS, Varley GA, Krachmer JH. Development of keratoconus after contact lens wear. Patient characteristics. Arch Ophthalmol. 1990 Apr;108(4):534-8.
43. Mazzotta C, Balestrazzi A, Traversi C, et al. Treatment of progressive keratoconus by riboflavin-UVA-induced cross-linking of corneal collagen; ultrastructural analysis by Heidelberg Retinal Tomograph II in vivo confocal microscopy in humans. Cornea. 2007 May;26(4):390-7.
44. Meek KM, Tuft SJ, Huang Y, et al. Changes in collagen orientation and distribution in keratoconus. Invest Ophthalmol Vis Sci. 2005. 2005 Jun;46(6):1948-56.
45. Wollensak G, Spoerl E, Seiler T. Riboflavin/ultraviolet-a-induced collagen crosslinking for the treatment of keratoconus. Am J Ophthalmol. – 2003 May;135(5):620-7.
46. Wollensak G, Spoerl E, Seiler T.. Stress-strain measurements of human and porcine corneas after riboflavinultraviolet – A-induced cross-linking. J Cataract Refract Surg. 2003 Sep;29(9):1780-5.
47. Werner LP, Issid K, WernerL, et al. Salzmann's corneal degeneration associated with epithelial basement membrane dystrophy. Cornea. 2000 Jan;19(1):121-3.
48. Winchester K, Mathers WD, Sutphin JE, et al. Diagnosis of Acanthamoeba keratitis in vivo with confocal microscopy. Cornea. 1995 Jan;14(1):10-7.

The authors declare no conflict of interest.

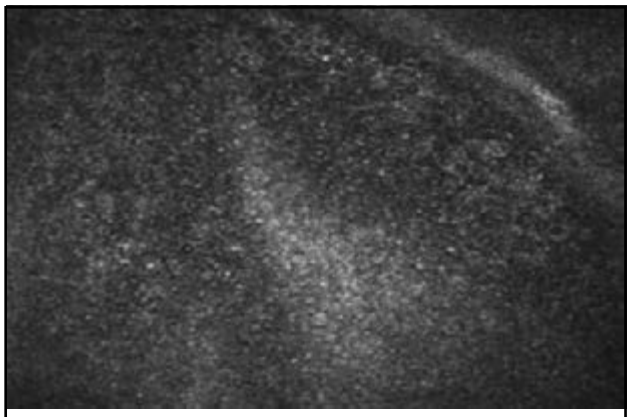

Fig. 1. Microscopic image of the corneal epithelium at 7 days after corneal collagen crosslinking

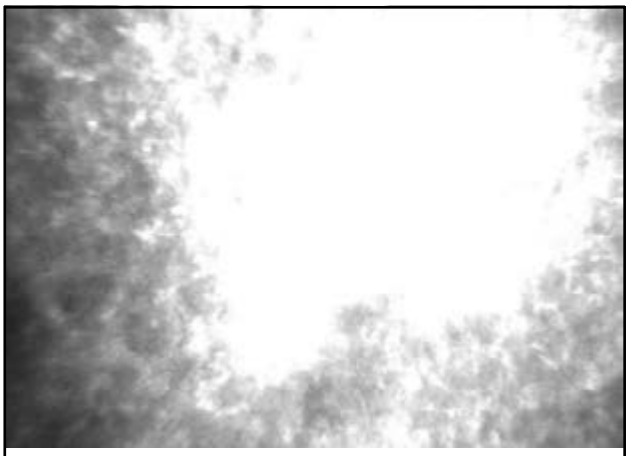

Fig. 4. Fibroplastic activity in the stroma of the cornea at 2 days after corneal collagen crosslinking

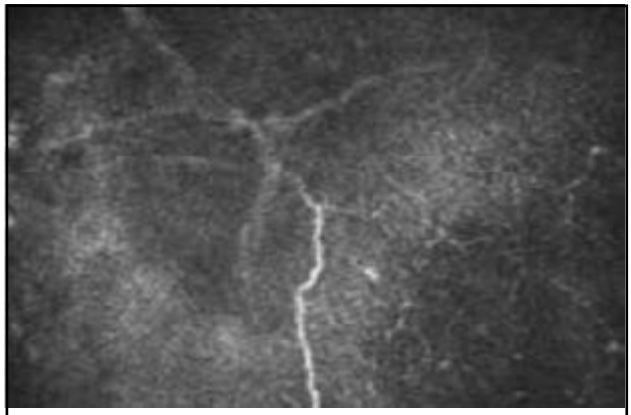

Fig. 2. Hyperreflective areas in the Bowman membrane at 7 days after corneal collagen crosslinking

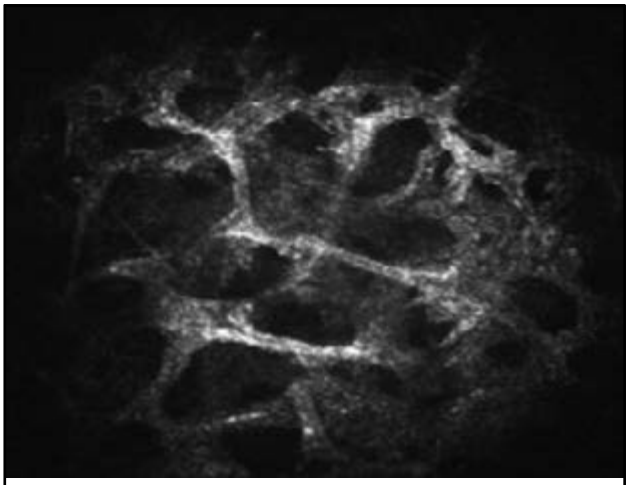

Fig. 5. Honeycomb-like appearance of the anterior stroma with no visualized nuclei at 7 days after corneal collagen crosslinking

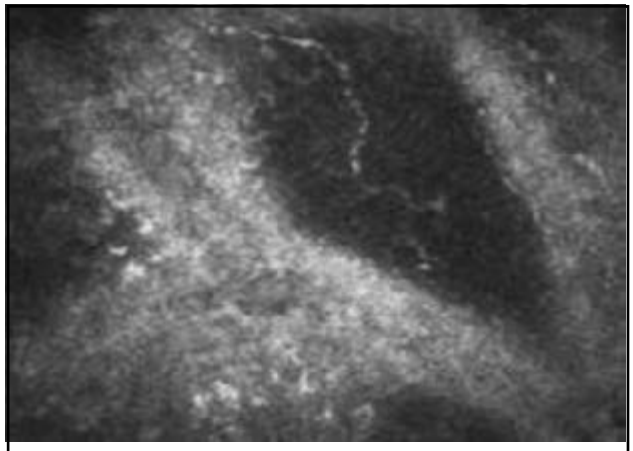

Fig. 3. Bright reflective areas in the Bowman membrane at 7 days after corneal collagen crosslinking

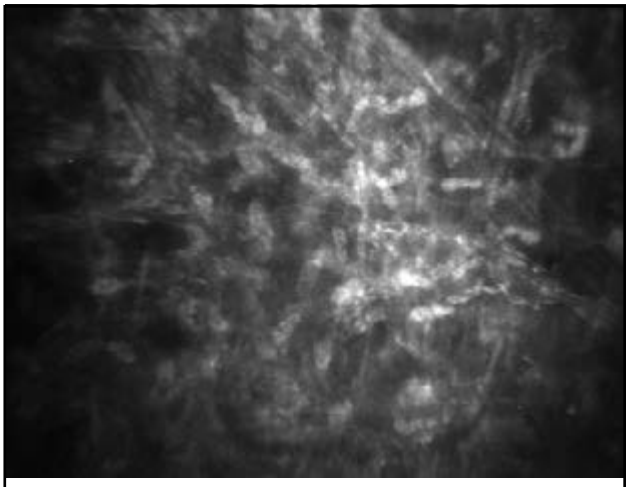

Fig. 6. Stromal opacity, apoptotic keratocytes and collagen fibres, and foci of hypocellularity at 7 days after corneal collagen crosslinking

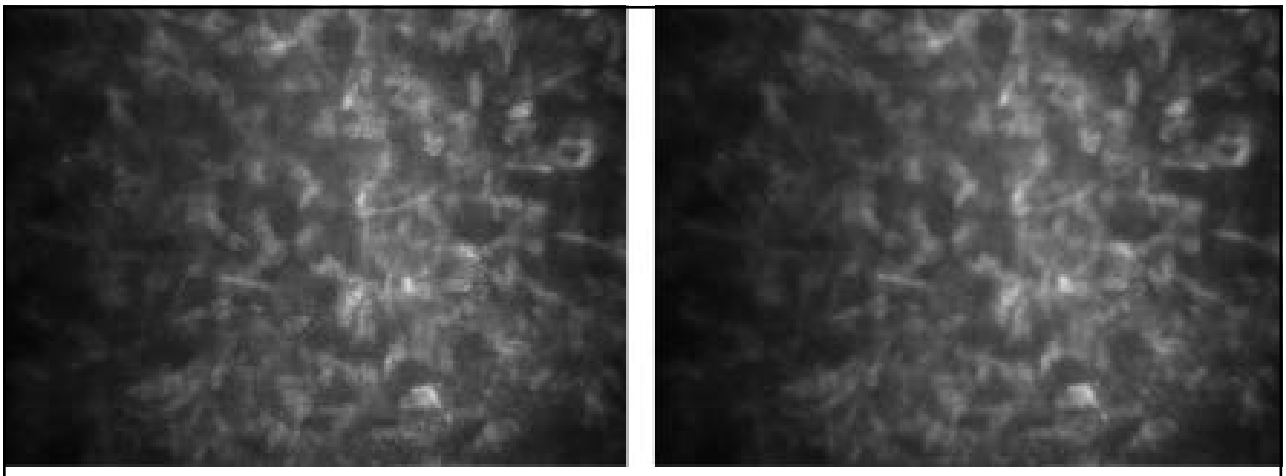

Fig. 7a,b. Decreased size of stromal meshwork and renewal of keratocytes at one month after corneal collagen crosslinking

Fig. 8. Active renewal of keratocytes at three months after corneal collagen crosslinking

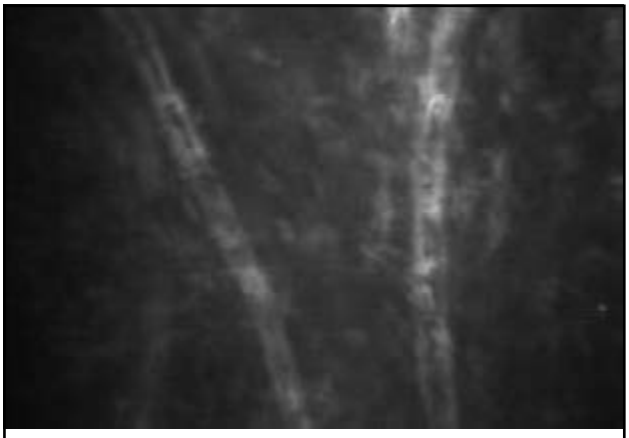

Fig. 10. Corneal structure approached the norm at 12 months after corneal collagen crosslinking

Fig. 9. Ongoing restoration of stromal structure at six months after corneal collagen crosslinking